AD-A018748

AD-A018 748

AD

FA-TM-75054

NORMAL FUZE IMPACT AND PERFORATION

LPL

August 1975

Approved for public release; distribution unlimited.
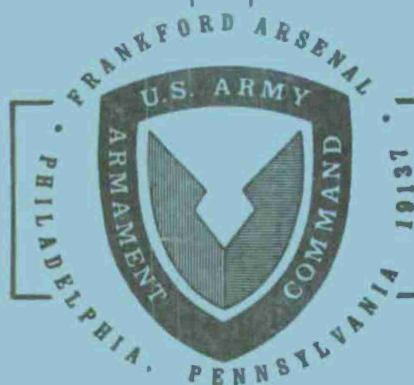
Pitman-Dunn Laboratory

# U.S. ARMY ARMAMENT COMMAND
## FRANKFORD ARSENAL
### PHILADELPHIA, PENNSYLVANIA 19137

DISPOSITION INSTRUCTIONS

| REPORT DOCUMENTATION PAGE | | READ INSTRUCTIONS<br>BEFORE COMPLETING FORM |
|---|---|---|
| 1. REPORT NUMBER<br><br>FA-TM-75054 | 2. GOVT ACCESSION NO. | 3. RECIPIENT'S CATALOG NUMBER |
| 4. TITLE *(and Subtitle)*<br><br>NORMAL FUZE IMPACT AND PENETRATION | | 5. TYPE OF REPORT & PERIOD COVERED<br><br>Technical Research Report |
| | | 6. PERFORMING ORG. REPORT NUMBER |
| 7. AUTHOR(s)<br><br>P. GORDON<br>F. LEE<br>M. SCHWARTZ | | 8. CONTRACT OR GRANT NUMBER(s) |
| 9. PERFORMING ORGANIZATION NAME AND ADDRESS<br><br>FRANKFORD ARSENAL<br>Attn: SARFA-PDM-E<br>Philadelphia, PA 19137 | | 10. PROGRAM ELEMENT, PROJECT, TASK<br>AREA & WORK UNIT NUMBERS<br>AMCMS CODE: 3653.5000.204<br>DA PROJ: 1W662616AH77 |
| 11. CONTROLLING OFFICE NAME AND ADDRESS<br><br>FRANKFORD ARSENAL | | 12. REPORT DATE<br><br>August 1975 |
| | | 13. NUMBER OF PAGES<br><br>25 |
| 14. MONITORING AGENCY NAME & ADDRESS(*if different from Controlling Office*) | | 15. SECURITY CLASS. (*of this report*)<br><br>UNCLASSIFIED |
| | | 15a. DECLASSIFICATION/DOWNGRADING<br>SCHEDULE    N/A |
| 16. DISTRIBUTION STATEMENT (*of this Report*)<br><br>Approved for public release; distribution unlimited. | | |
| 17. DISTRIBUTION STATEMENT (*of the abstract entered in Block 20, if different from Report*) | | |
| 18. SUPPLEMENTARY NOTES | | |

19. KEY WORDS (*Continue on reverse side if necessary and identify by block number*)

Impact
Perforation
Stress distribution
Plugging
Petalling

Stress wave
Projectile

20. ABSTRACT (*Continue on reverse side if necessary and identify by block number*)

A model for the penetration through a thin target by a fuzed projectile at normal incidence was developed. It was assumed that the penetration mechanisms were plugging followed by petalling. From this model the force and stress distributions acting on the fuze were plotted. It was found that the major stress on the fuze was the longitudinal component due to plugging. The effects of petalling were negligible. The forces and stresses were found to be proportional to the square of the impact velocity.

DD $_{1\ JAN\ 73}^{FORM}$ 1473    EDITION OF 1 NOV 65 IS OBSOLETE
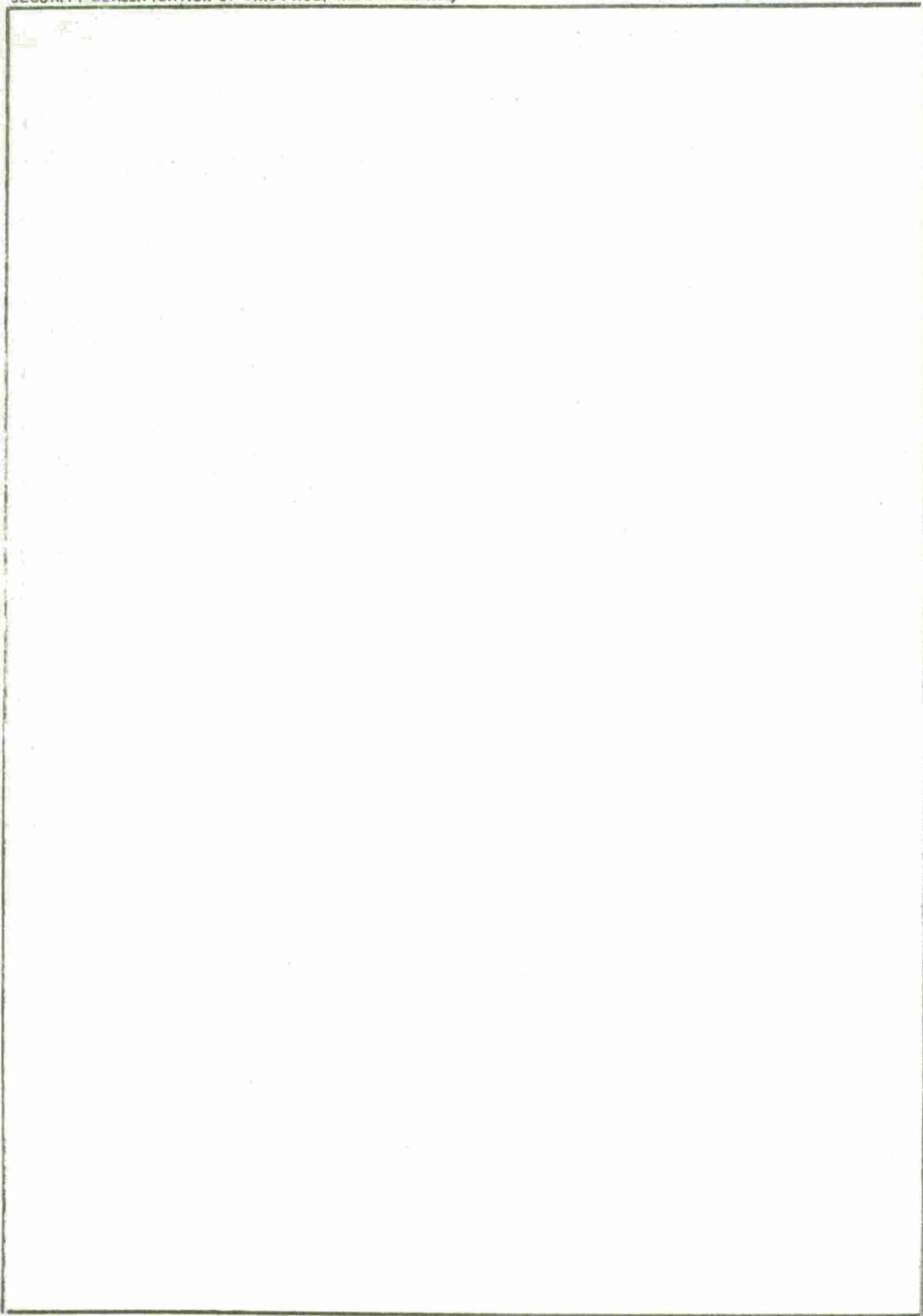
# TABLE OF CONTENTS

## LIST OF ILLUSTRATIONS

### Figure

1

# GLOSSARY

A    – Area* of projectile upon which forcing function acts in.$^2$, Equation 5

A'   – dA/dx, Equation 17

C    – Constant, Equation 4

c    – Wave speed = $\sqrt{E/\rho_1}$, ft/sec, Equation 17

D    – Constant in., Equation 4

E    – Elastic modulus, $lb_f/in.^2$, Equation 16

F    – Force$^\dagger$ acting on projectile, $lb_f$, Equation 1

$h_o$   – Thickness of target plate, in., Equation 1

k    – Constant of integration, Equation 21

n    – Number of petals, Equation 2

R    – Radius of end of projectile, in., Equation 29

S    – Shear force on plug, psi, Equation 29

s    – Surface area of projectile, in.$^2$, Equation 5

t    – Time, sec, Equation 15

u    – Displacement, in., Equation 15

$v_s$   – Striking velocity of projectile, in./sec, Equation 1

x    – Distance from tip of projectile, in., Equation 1

$Y_o$  – Compressive yield strength, $lb_f/in.^2$, Equation 29

$Y(x)$ – Radius of projectile at corresponding values of x, in., Equation 4

z    – Penetration of fuze into target, ft, Equation 29

$\ddot{z}$   – Acceleration in the z-direction, $ft/sec^2$, Equation 31

*The subscript $_o$ denotes evaluation at the end of projectile.

†The subscripts A and R denote the axial and radial direction, respectively.

$\alpha$     -   Half angle of projectile nose cone, $^\circ$, Equation 1

$\beta, \gamma$    -   Constants, Equation 18

$\rho$     -   Mass density of target, $lb_f\text{-}sec^2/in.^4$, Equation 1

$\rho_1$     -   Mass density of projectile, $lb_f\text{-}sec^2/in.^4$, Equation 15

$\sigma$     -   Stress[†] distribution in projectile, psi, Equation 12

## INTRODUCTION

This work was performed under the Fuze Technology Program AH77. The purpose of this study was to determine the stress distribution in a generalized fuze by means of an analytical representation of the external and internal stresses experienced by the fuze while penetrating a thin target.

In this study it was assumed that penetration through a thin target is accomplished first by plugging and then by petalling. This assumption is similar to that of Zaid and Paul[1-3], who, in their work, described the failure mechanism associated with a thin target impacted by a blunted conical projectile in the same manner. The model developed for plugging assumes that a disk or plug is sheared from the target early in the penetration process, and the resulting normal force between projectile and plug causes a stress wave to be generated at the impact face which subsequently moves at sonic velocity down the projectile. Petalling, which produces the force and stress distributions on the surface of the projectile, was analyzed using the model of Zaid and Paul ; and some of the mathematics used in this report is taken from Reference 1. The acutal projectile shape in this study is a cone with a small spherical tip; however, in order to avoid infinite stresses associated with a point, i.e., the contact point of the projectile tip with the target, the assumed shape was taken to be a truncated cone (Figure 1). It was assumed that the material at the tip rapidly deforms plastically an instant after impact so that the truncation approximateion is reasonable.

## ANALYSIS

The stress wave propagation was assumed to be one-dimensional. General algebraic equations were derived for the force and stress functions, and numerical values based on ballistic data were calculated and plotted. No attempt has been made to superimpose the effects of petalling and plugging, nor to consider stress wave reflections from the projectile or target surfaces.

1

M. Zaid, and B. Paul, Mechanics of High Speed Projectile Perforation, J. Franklin Inst., 264, 1957, 117.

2

M. Zaid, and B. Paul, Normal Perforation of a Thin Plate by a Truncated Conical Projectile, J. Franklin Inst., 1958, 317.

3

M. Zaid, and B. Paul, Oblique Perforation of a Thin Plate by a Truncated Conical Projectile, J. Franklin Inst., 1959, 24.
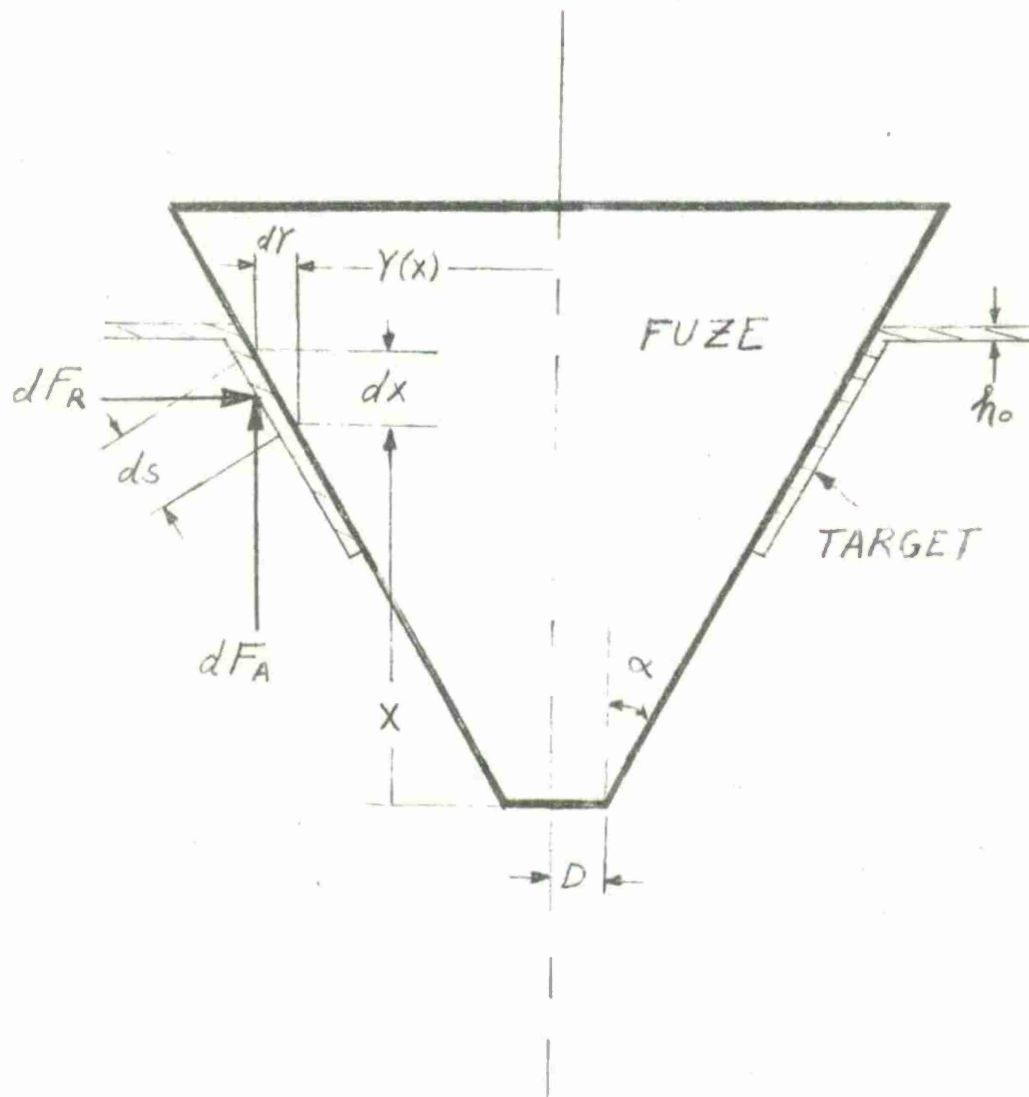
Figure 1.   Petalling of Target by Fuze

A. Petalling

   1. Surface Force Distribution Along Length of Projectile.

   From Reference 1, the axial and radial forces (Figure 1) were shown to be

$$F_A = 2\pi\rho h_o \, v_s^2 \, \tan^2 \alpha \, \sin \alpha \, x, \qquad (1)$$

$$F_R = (1/n)2\pi\rho h_o \, \tan^3 \alpha \, (1-\sin \alpha) \, v_s^2 \, x; \qquad (2)$$

and the resultant force is

$$F = (F_A^2 + F_R^2)^{\frac{1}{2}} \qquad (3)$$

The value of n has been determined experimentally, and, for most cases, 5 is the predominate value. In these calculations, three different values of n were used to show the range of F and σ. These values were n = 4, 5, and 6. As shown in Equations 1 and 2, the axial force is independent of n, but the radial force is inversely proportional to n. However, both forces are linearly proportional to x.

   For this analysis the fuze was taken to be a solid truncated cone of aluminum with a total length of 1.305 inches and a front and rear radii of 0.100 inches and 0.338 inches respectively. The semi-cone angle was calculated to be 11.5°. Figures 2, 3, and 4 show the axial, radial and resultant forces, respectively, plotted as a function of distance from the tip of the fuze for perforation of an aluminum target 0.06 inches thick.

   2. Surface Stress Distribution Along Length of Projectile

   The truncated cone shape of the projectile can be expressed mathematically as,

$$Y(x) = Cx + D, \qquad (4)$$

where the values of C and D are found from geometrical considerations. For the projectile of this study C = 0.203 and D = 0.100 inches.

[1] M. Zaid, and B. Paul, Mechanics of High Speed Projectile Perforation, J. Franklin Inst., 264, 1957, 117.
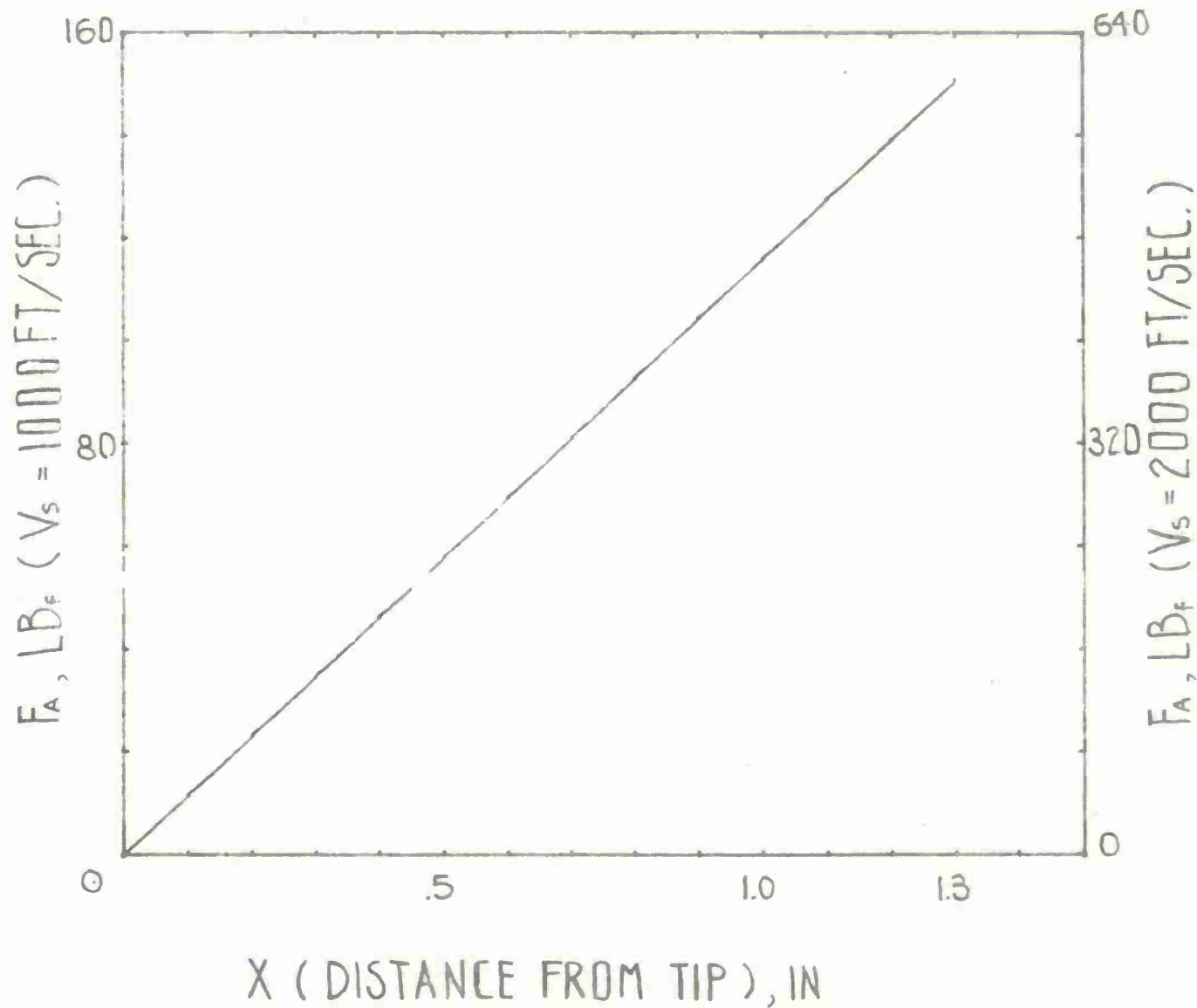
Figure 2.   Axial Force on Fuze Surface Due to Petalling versus
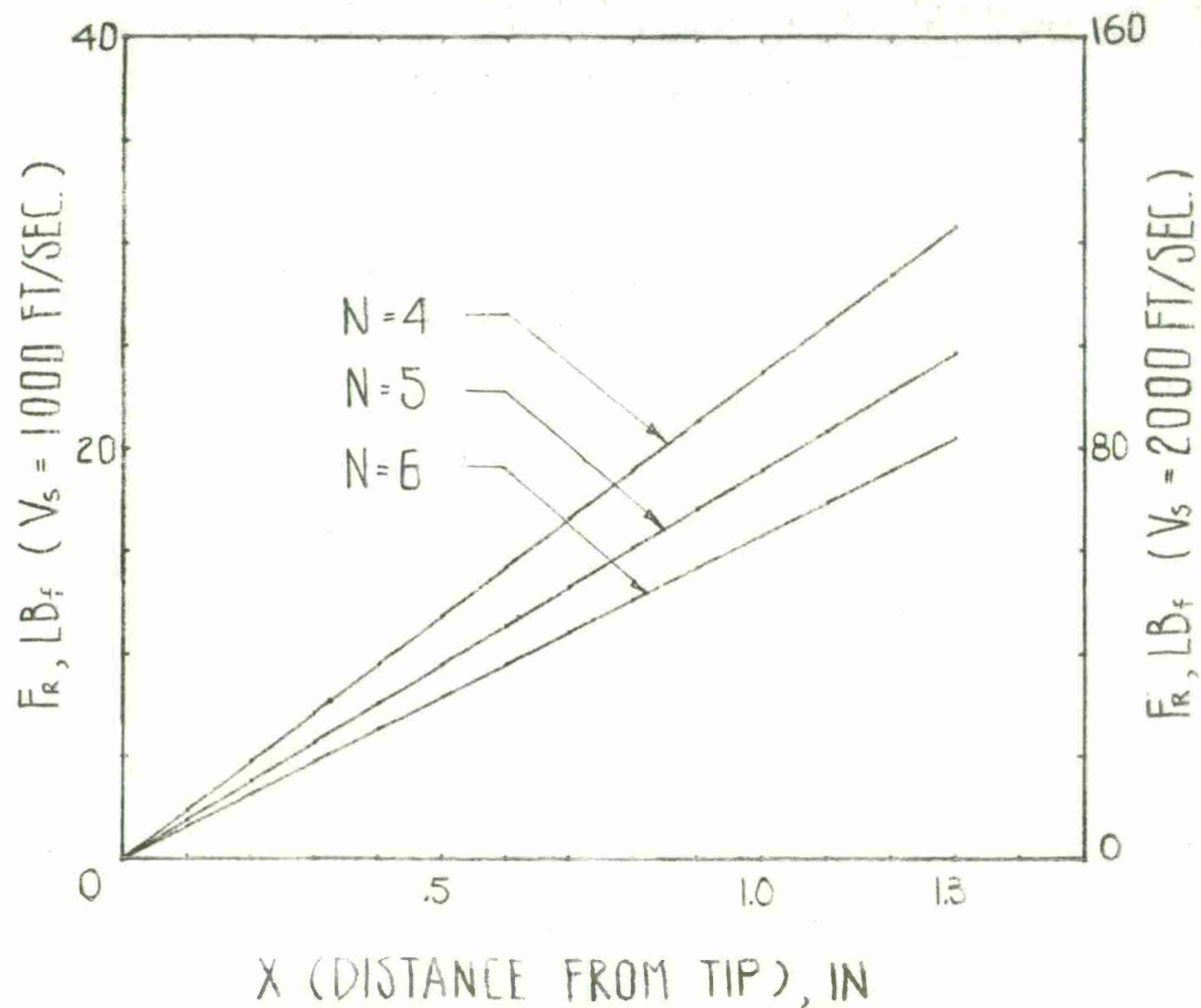Distance from Impact Surface

Figure 3. Radial Force on Fuze Surface Due to Petalling versus Distance from Impact Surface
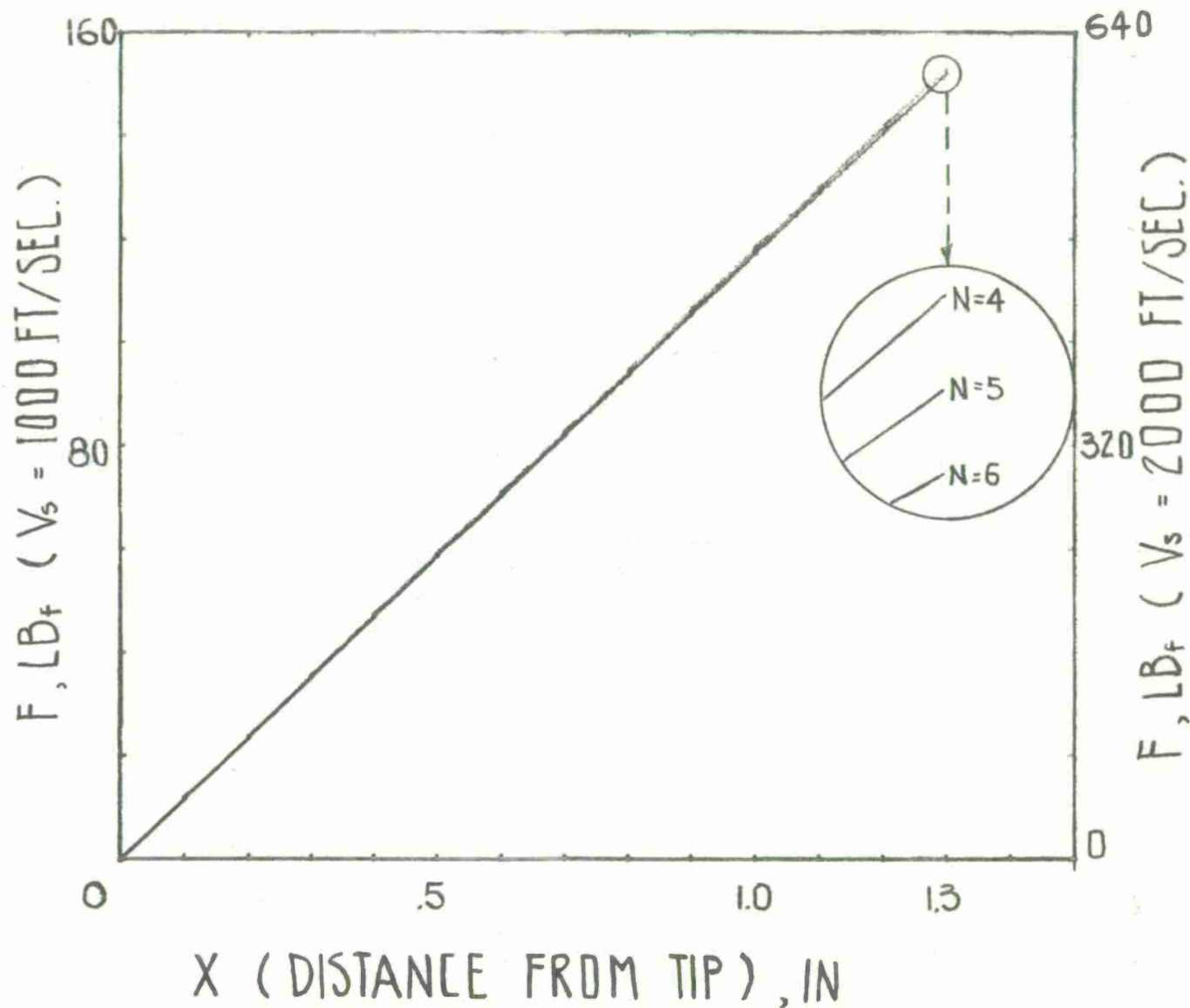
Figure 4.    Resultant Force on Fuze Surface Due to Petalling versus
Distance from Impact Surface

The elemental surface area upon which the axial force acts is

$$dA_R(x) = 2\pi Y(x) \ ds \ \sin \alpha, \tag{5}$$

and similarly, the elemental surface area upon which the radial force acts is

$$dA_A(x) = 2\pi Y(x) \ ds \ \cos \alpha, \tag{6}$$

Since

$$ds = \left[1 + (dY/dx)^2\right]^{\frac{1}{2}} dx, \tag{7}$$

Equations 5 and 6 become

$$dA_A(x)/dx = 2\pi Y(x) \left[1 + (dY/dx)^2\right]^{\frac{1}{2}} \sin \alpha, \text{ and} \tag{8}$$

$$dA_R(x)/dx = 2\pi Y(x) \left[1 + (dY/dx)^2\right]^{\frac{1}{2}} \cos \alpha. \tag{9}$$

Upon substitution of $dY/dx$ from Equation 4, Equations 8 and 9 become

$$dA_A(x)dx = 2\pi Y(x) \left[1 + C^2\right]^{\frac{1}{2}} \sin \alpha, \text{ and} \tag{10}$$

$$dA_R(x)/dx = 2\pi Y(x) \left[1 + C^2\right]^{\frac{1}{2}} \cos \alpha. \tag{11}$$

The definition of stress is

$$\sigma = dF/dA = dF/dx \div dA/dx. \tag{12}$$

From Equations 1, 2, 10 and 11, the axial and radial stresses are

$$\sigma_A = \rho h_o \ v_s^2 \ \tan^2 \alpha / \left[Cx + D\right]\left[1 + C^2\right]^{\frac{1}{2}}, \text{ and} \tag{13}$$

$$\sigma_R = \rho h_o \ v_s^2 \ \tan^3 \alpha \ (1-\sin \alpha)/n(Cx + D)(1 + C^2)^{\frac{1}{2}} \cos \alpha. \tag{14}$$

10

Equations 13 and 14 show that the stress in the projectile decreases as the distance from the tip increases. Figures 5 and 6 are plots of the axial stress and radial stress, respectively, as a function of distance from the tip of the fuze.

B. Plugging

The idealized fuze shown in Figure 7 is assumed to be an elastic bar with a modulus (E) and variable cross-sectional area (A). It is also assumed that the impact stress generates a stress wave which is longitudinal, one-dimensional and planar while propagating down the fuze. Equilibrium of the fuze requires that

$$\frac{\partial}{\partial x}(\sigma A) - \rho_1 A \frac{\partial^2 u}{\partial t^2} = 0, \tag{15}$$

in which $u$ and $\sigma$ are functions of $x$ and $t$, and $A$ is a function of $x$ alone.

The relation between stress and strain is described by the linear Hooke's law

$$\sigma = E \frac{\partial u}{\partial x}, \tag{16}$$

where $\frac{\partial u}{\partial x}$ is the longitudinal strain.

Eliminating $\sigma$ between Equations 15 and 16 leads to

$$\frac{\partial^2 u}{\partial x^2} + \frac{\partial u}{\partial x}\left(\frac{A'}{A}\right) - \frac{1}{c^2} \frac{\partial^2 u}{\partial t^2} = 0, \tag{17}$$

which is the fundamental equation describing elastic wave propagation in the fuze. Considering the simplicity of the one dimensional assumptions made above, a complete solution of Equation 17 is unwarranted. However, a solution of Equation 17, valid at the moving wavefront, is required and is given below.

The general theory for moving wavefronts is presented in Reference 4. The results of that reference are used herein without detailed re-derivation.

---

[4]R. Karpp, and P.C. Chou, The Method of Characteristics in Dynamic Response of Materials to Intense Impulsive Loading, Ed. by P.C. Chou, and A.K. Hopkins, Air Force Materials Laboratory, W-P AFB, Ohio, 1972. pp 283-291.
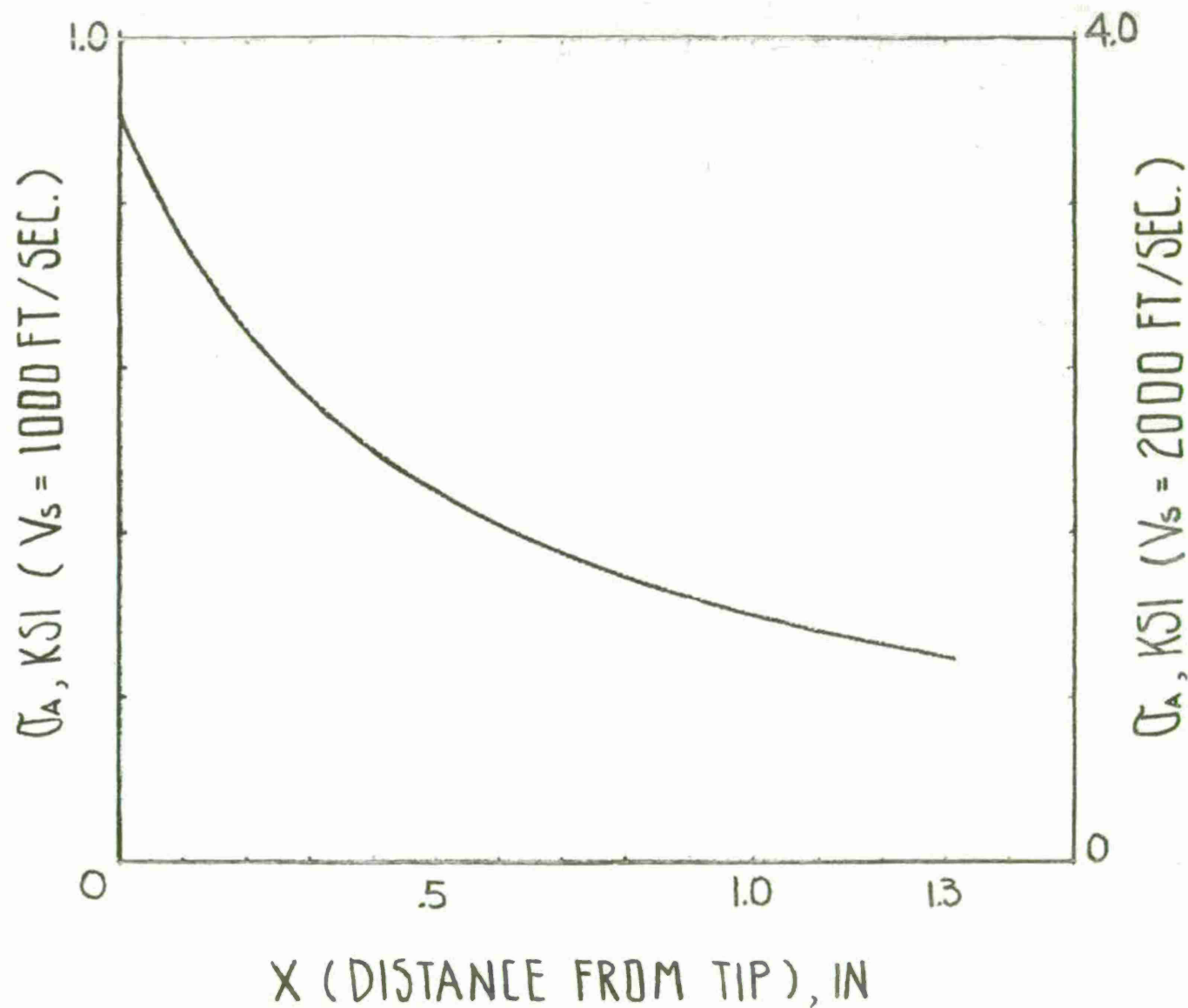
Figure 5. Axial Stress on Fuze Surface Due to Petalling versus
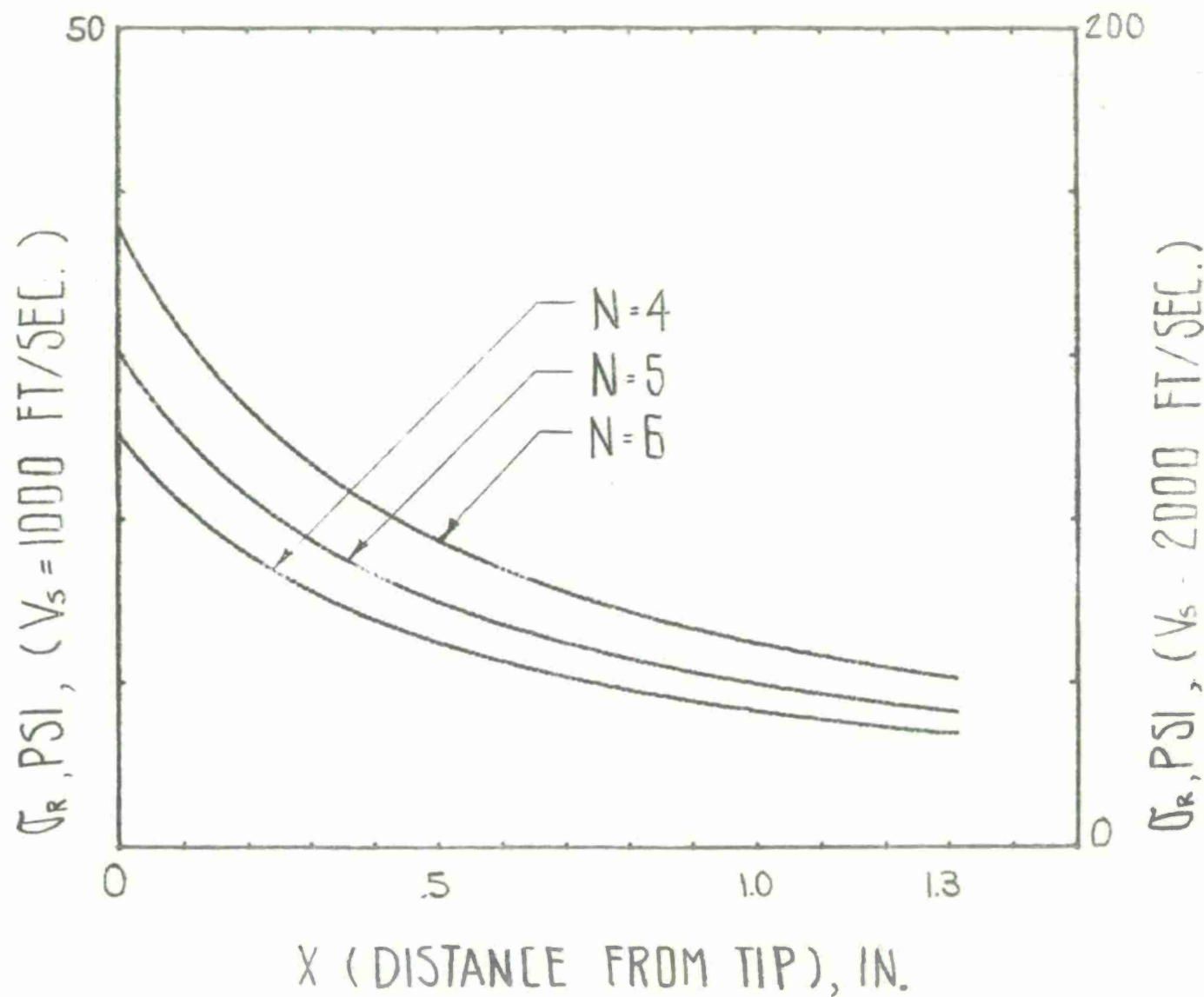Distance from Impact Surface

12

Figure 6. Radial Stress on Fuze Surface Due to Petalling versus
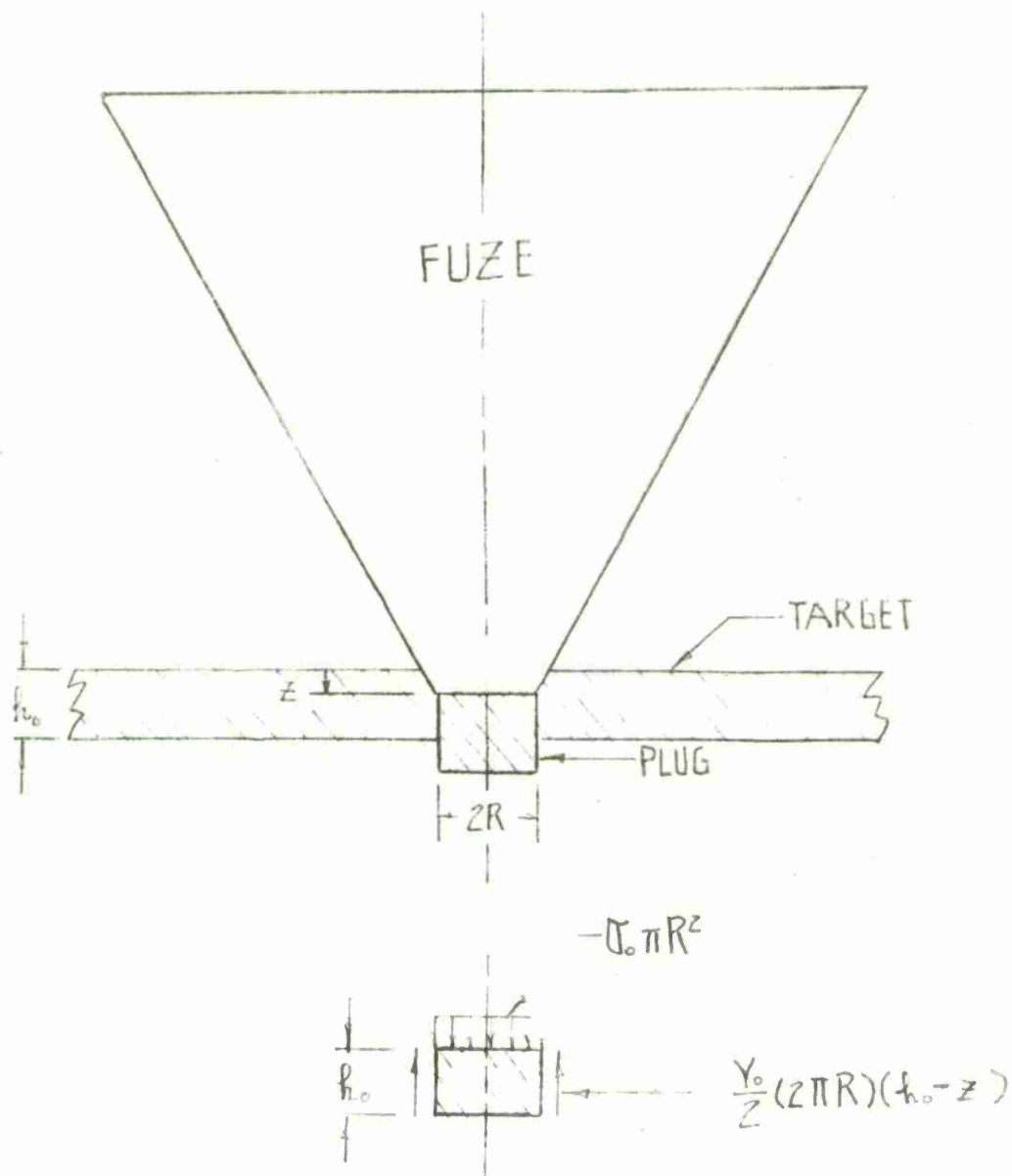Distance from Impact Surface

Figure 7. Plugging of Target by Blunted End of Fuze

14

It was shown[4] that for any linear wave equation of the form

$$\frac{\partial^2 u}{\partial x^2} - \frac{1}{C^2}\frac{\partial^2 u}{\partial t^2} = \gamma u + \beta\frac{\partial u}{\partial x} \ , \tag{18}$$

where $\gamma$ and $\beta$ are either constants or, at most functions of $x$ and $t$, that the jumps in $\frac{\partial u}{\partial x}$ and $\frac{\partial u}{\partial t}$ are governed by the differential equations.

$$\frac{d}{dx}\left[\frac{\partial u}{\partial x}\right] = (\beta/2)\left[\frac{\partial u}{\partial x}\right] \ , \text{ and} \tag{19}$$

$$\frac{d}{dx}\left[\frac{\partial u}{\partial t}\right] = (-c\beta/2)\left[\frac{\partial u}{\partial t}\right] . \tag{20}$$

In Equations 19 and 20, the symbol $\left[f\right]$ denotes the jump of the enclosed quantity $f$, which physically represents the difference between the values of $f$ immediatey behind and immediately in front of the wave front.

Integrating Equations 19 and 20 yields

$$\left[\frac{\partial u}{\partial x}\right] = k \ \exp(\tfrac{1}{2}\!\int\!\beta x) \ , \tag{21}$$

$$\left[\frac{\partial u}{\partial t}\right] = -ck \ \exp(\tfrac{1}{2}\!\int\!\beta dx) \ . \tag{22}$$

The above equations are now applied to Equation 17. Comparing Equations 18 and 17 we see that $\gamma = 0$ and

$$\beta = -A'(x)/A(x) \ . \tag{23}$$

Using Equations 21 to 23 we have

$$\frac{\partial u}{\partial x} = k \ A^{-\frac{1}{2}}, \text{ and} \tag{24}$$

4

R. Karpp, and P.C. Chou, The Method of Characteristics in Dynamic Response of Materials to Intense Impulsive Loading, Ex. by P.C. Chou, and A.K. Hopkins, Air Force Materials Laboratory, W-P AFB, Ohio, 1972. pp 283-291.

$$\frac{\partial u}{\partial t} = -c \left[ \frac{\partial u}{\partial x} \right] . \tag{25}$$

The constant $k$ may be evaluated by noting that at $x = 0 = t$ a stress magnitude $-\sigma_O$ is applied. The final results are thus;

$$\left[ \frac{\partial u}{\partial x} \right] = -(\sigma_O/E)(A_O/A)^{\frac{1}{2}} , \tag{26}$$

$$\left[ \sigma \right] = -\sigma_O(A_O/A)^{\frac{1}{2}} , \text{ and} \tag{27}$$

$$\left[ \frac{\partial u}{\partial t} \right] = -c \left[ \frac{\partial u}{\partial x} \right] . \tag{28}$$

As can be seen from the above, the strain, stress, and particle velocity decrease inversely as the square root of the area.

It should be emphasized that the above results in Equations 26 to 28 are vaild only at the leading wavefront, $x = ct$, and for values of time less than the time required for one transit, i.e., $h_O/c$.

In order to determine $\sigma$ from Equation 27, $\sigma_O$ was calculated first. $\sigma_O$ was calculated from the forces acting on the plug as shown in Figure 7. Using the analysis in Reference 5, the shear force resisting penetration is

$$S = - (\tfrac{1}{2})Y_O(2\pi R)(h_O-z), \tag{29}$$

where $Y_O$ is the yield strength in simple compression.

It was assumed that the plug and fuze do not separate until penetration is complete. Thus a force

$$F = \sigma_O\pi R^2 , \tag{30}$$

---

[5]

P.F. Gordon, Temperature Distribution in Impacted Plates, M73-6-1, March 1973, Frankford Arsenal, Phila., Pa., p. 5.

16

acts on both fuze and plug.  Equating the forces on the plug to the inertia of the plug yields

$$\sigma_O = (1/\pi R^2) \left[ \rho \pi R^2 h_O \ddot{z} + (\tfrac{1}{2})(2\pi R)(h_O - z) \right] . \tag{31}$$

It was assumed for simplicity that the acceleration on the plug was constant during penetration and equal to

$$\ddot{z} = \frac{\Delta v}{\Delta t} \cong \frac{v_s}{\Delta t} , \tag{32}$$

where $\Delta t$ is the transit time for the target thickness in free air.

The final values of $\sigma_O$ to be used in Equation 27 were obtained by averaging the two values of $\sigma_O$ obtained from Equation 31 by taking $z = 0$ and $z = h_O$.  The final values are $\sigma_O = 52,300$ psi for $v_s = 1000$ fps and $\sigma_O = 164,000$ psi for $v_s = 2000$ fps.  The nondimensional stress is plotted from Equation 27 as a function of distance down the fuze as shown in Figure 8.  The initial impact values of the stress $\sigma$ occur at $x = 0$ where $\sigma/\sigma_O = 1$.  Note that by the time the wave reaches the end of the fuze, whose length is 1.3", $\sigma/\sigma_O \cong 0.28$ and the stress has decreased to 14,500 psi (at 1000 fps) and 45,900 psi (at 2000 fps).

The static yield strength of the fuze is about 50,000 psi.  Thus the $\sigma_O$ values given above exceed the static yield strength of the material.  However, when a metal is loaded dynamically, the yield point is elevated.  Also some of the plastic energy will be used in blunting the nose.  These two facts, coupled with the strong attenuation discussed above, and the very short time for perforation of a thin target, indicate that only a small amount, if any, of plastic flow can occur past the vicinity of the crushed end.

## CONCLUSIONS

From this study the following conclusions can be made:

1.  Both the axial and radial surface forces (stresses) vary directly (inversely) with the distance from the impact end of the projectile.

2.  Both the radial surface forces and stresses vary inversely with the number of petals produced.
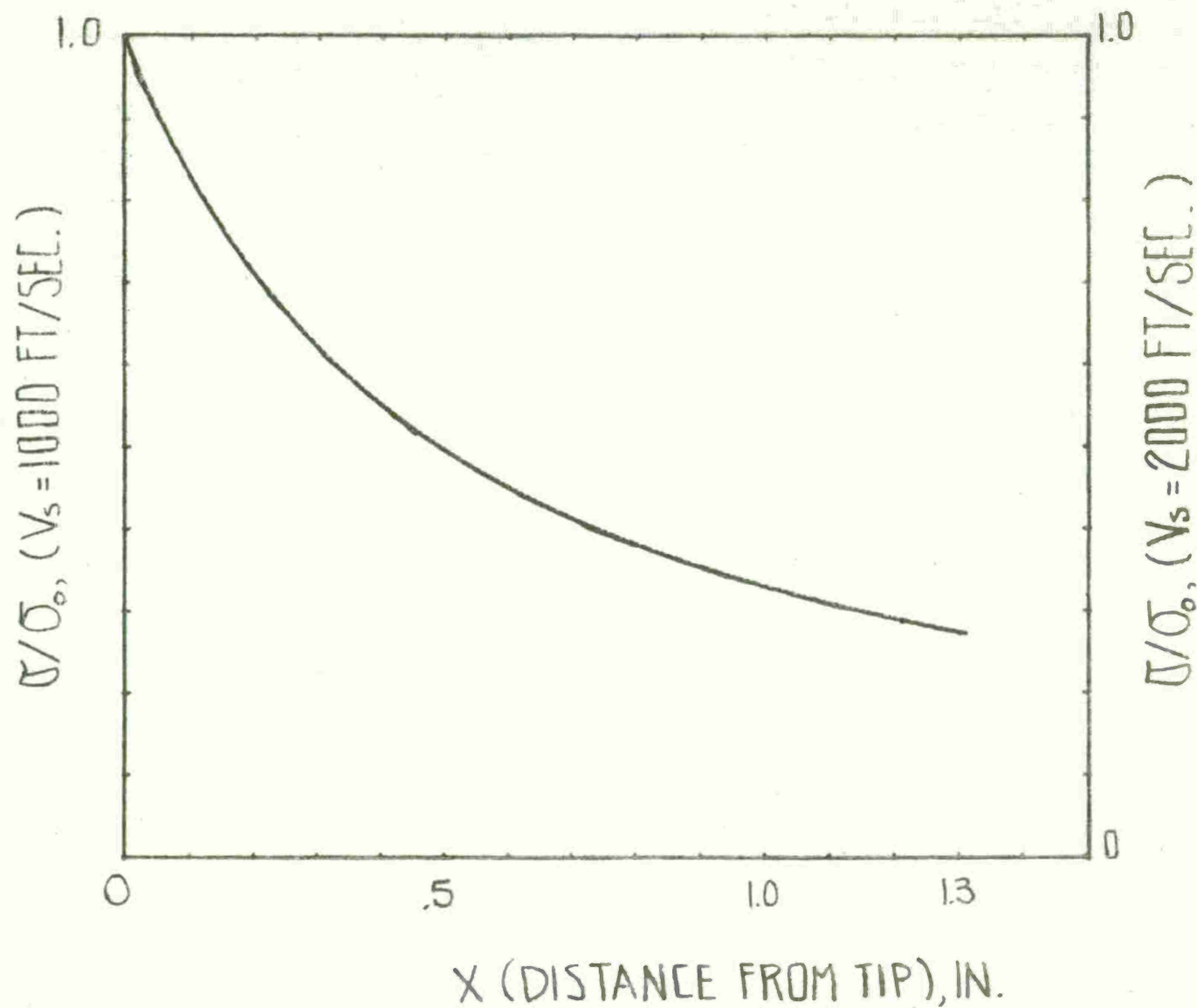
17

Figure 8. Dimensionless Stress Due to Plugging versus Distance from Impact Surface

3.  The internal stresses due to plugging decrease inversely as the square root of the cross-sectional area.

4.  All of the forces and stresses vary directly as the square of the impacting velocity.

5.  For the projectile geometry and velocities studied in this report the radial components of surface forces and stresses are small, amounting to about 20 percent and 5 percent, respectively, of the total effects.  The number of petals produced has a negligible effect on the resultant surface force.

6.  The major stress on the generalized fuze is that due to plugging. At the impact end this stress is 52,000 psi for an incident velocity of 1000 fps and 164,000 psi for an incident velocity of 2000 fps.  The stresses due to petalling amount to only a few percent of that due to plugging.

# REFERENCES

1. M. Zaid, and B. Paul, Mechanics of High Speed Projectile Perforation, J. Franklin Inst., 264, 1957, 117.

2. M. Zaid, and B. Paul, Normal Perforation of a Thin Plate by Truncated Projectiles, J. Franklin Inst., 1958, 317.

3. M. Zaid, and B. Paul, Oblique Perforation of a Thin Plate by a Truncated Concial Projectile, J. Franklin Inst., 1959, 24.

4. R. Karpp, and P.C. Chou, The Method of Characteristics in Dynamic Response of Materials to Intense Impulsive Loading, Ed. by P.C. Chou, and A.K. Hopkins, Air Force Materials Laboratory, W-P AFB, Ohio, 1972, pp 283-291.

5. P.F. Gordon, Temperature Distribution in Impacted Plates, M73-6-1, March 1973, Frankford Arsenal, Phila., Pa., p. 5.

Office Chief of Research &
    Development
Department of the Army
Attn:  DARD-ARP-T,
        Dr. Thomas Sullivan
Washington, DC  20315

Advanced Research & Technology
    Division
Department of Defense
Washington, DC  20301

Commander
US Army Missile Command
Huntsville, AL  35809

1 Attn:  Doc & Tech Info Branch

1 Attn:  AMSMI-RSM
        Mr. E. Wheelahan

Commander
US Army Electronics Command
Attn:  Tech Info Division
Fort Monmouth, NH  07703

Commander
US Army Aviation Materiel Command
P.O. Box 209, Main Office
St. Louis, MO  63166

1 Attn:  Technical Info Division

1 Attn:  Small Arms Systems Agency

Commander
Rocky Mountain Arsenal
Attn:  Technical Info Division
Denver, CO  80240

Commander
US Army Edgewood Arsenal
Attn:  Dr. E. Metcalfe
Edgewood, MD  21005

Commander
US Army Watervliet Arsenal
Watervliet, NY  12189

Commander
US Army Materiel Command
5001 Eisenhower Avenue
Alexandria, VA  22304

2 Attn:  AMCDL-CS,
        Chief Scientist

1 Attn:  AMCDL,
        Deputy for Laboratories

1 Attn:  AMCRD,
        Deputy Director for Plans

1 Attn:  AMCRD-F,
        Air Systems Division

1 Attn:  AMCRD-E,
        Engineering Division

1 Attn:  AMCRD-I,
        Foreign Science & Tech
            Division

1 Attn:  AMCRD-J,
        Individual Soldier Division

1 Attn:  AMCRD-M,
        Missile Systems Division

1 Attn:  AMCRD-TC,
        Mr. L. Croan, Bldg T-7

1 Attn:  AMCRD-G,
        Surface Systems Division

1 Attn:  AMCRD-U,
        Test & Evaluation Division

1 Attn:  AMCRD-W,
        Weapons Munitions Systems
            Division

Commander
US Army Redstone Arsenal
Attn:  Technical Info Division
Huntsville, AL  35809

Commander
US Army Test & Evaluation Command
Aberdeen Proving Ground, MD   21005

1 Attn:   STEAP-DS-TU,
          Mr. W. Pless

1 Attn:   STEAP-MT-TI,
          Mr. Hines

Commander
US Army Materials & Mechanics
   Research Center
Watertown, MA   02172

1 Attn:   Technical Info Division

1 Attn:   AMXMR-E,
          Dr. E.S. Wright

1 Attn:   AMXMR-TX

1 Attn:   AMXMR-ED,
          Mr. P. Riffin

1 Attn:   AMXMR-ED,
          Mr. K. Abbott

Commander (2)
Technical Library, Bldg 313
Aberdeen Proving Ground, MD   21005

Commander
US Army Rock Island Arsenal
Rock Island, IL   61201

1 Attn:   Technical Info Division

1 Attn:   SWERR-ST,
          Mr. Mayer
          ACT Project Director

Commander
Harry Diamond Laboratories
Attn:  AMXDO-TIB
Washington, DC   20438

Commander
US Army Research Office
Attn:  Dr. H. Davis
          Chief, Met & Cer Division
Box CM, Duke Station
Durham, NC   27706

Commander
US Army Lake City Army Ammunition
   Plant
Independence, MO   64056

1 Attn:   SARLC-ATD

2 Attn:   SARLC-ATD-TS,
          Mr. Elmer Finney

Commander
Naval Air Systems Command
Attn:  AIR 52031A, Mr. R. Schmidt
Washington, DC   20360

Commander
Naval Air Development Center
Attn:  Mr. Forrest Williams-MAN
          Aero Materials-Department
Johnsville, Warminster, PA   18974

Commandant
US Naval Weapons Laboratory
Dahlgren, VA   22448

Commander
US Naval Engineering Experimental
   Station
Attn:  Materials Laboratory, WCTRL-2
Annapolis, MD   21402

Commander
US Naval Ordnance Test Station
Attn:  Code 5557
China Lake, CA   93557

Commander
US Naval Ordnance Laboratory
Attn:  Code WM
Silver Spring, MD   20910

Commander
US Army Armament Command
Rock Island, IL  61201

1 Attn:  AMSAR-ASF,
         Field Service Division

1 Attn:  AMSAR-RD,
         Director, Research
         Development & Engineering
         Directorate

1 Attn:  AMSAR-RDF,
         Mr. Chesnov

1 Attn:  AMSAR-RDM,
         Systems Development
         Division, Chemical &
         Nuclear

1 Attn:  AMSAR-RDS,
         Engineering Support
         Division

1 Attn:  AMSAR-RDT,
         Concepts & Technology
         Division

1 Attn:  AMCPM-SA,
         Selected Ammunition

1 Attn:  AMCPM-VRF,
         Vehicle Rapid Fire
         Systems Division

1 Attn:  AMSAR-LMC,
         USMC Liaison Officer

1 Attn:  Systems Development
         Division, Conventional
         Ammunition

1 Attn:  Manufacturing Engineering
         Division

1 Attn:  Munitions Reliability
         Systems Division

Commander
US Army Picatinny Arsenal
Dover, NJ  07801

2 Attn:  SARPA,
         Scientific & Technical
         Information Branch

1 Attn:  SARPA,
         Technical Director

1 Attn:  SARPA-AD-DA3,
         Mr. Resiman
         ACT Coordinator

1 Attn:  SARPA-D,
         Director, Ammunition
         Engineering Directorate

1 Attn:  SARPA-DD,
         Chief, Ammunition
         Development Division

1 Attn:  SARPA-DP,
         Chief, Munitions
         Engineering Directorate

1 Attn:  SARPA-DF,
         Chief, Fuze Research &
         Engineering Division

1 Attn:  SARPA-V,
         Director, Feltman
         Research Laboratories

1 Attn:  SARPA-VP.
         Chief, Materials
         Engineering Laboratories

Commander
Naval Weapons Center
Attn:  Mr. P. Miller
China Lake, CA  93555

Commander
Aeronautical Systems Division
Attn:  Technical Info Division
Wright-Patterson AFB
Dayton, OH  45433

Commander
A.F. Armament Laboratories
Attn: DLOS
Eglin AFB, FL 32542

Commander
Air Research & Development Command
Andrews Air Force Base
Attn: RDRAA
Washington, DC 20025

Commander
US Army Hill Air Force Base
Attn: R. Hamilton
Ogden, UT

Director
Ballistic Research Laboratory
Aberdeen Proving Ground, MD 21005

1 Attn: Dr. Albert Eichelberger,
Technical Director

3 Attn: AMXBR-IB,
A. Baran,
ACT Coordinator

Chief
Bureau of Weapons
Department of the Navy
Washington, DC 20025

Naval Ships Systems Command
Department of the Navy
Attn: Code 03423

Director
US Naval Research Laboratory
Attn: Code 6300
Mr. W.S. Pellini
Washington, DC 20390

Office of Naval Research
Department of the Navy
Attn: Code 423
Washington, DC 20025

Chief
Bureau of Ships
Department of the Navy
Attn: Code 343
Washington, DC 20360

Chief
Bureau of Aeronautics
Department of the Navy
Washington, DC 20360

Director
Air Force Materials Laboratory
Research & Technology Division
Wright-Patterson AFB
Dayton, OH 45433

1 Attn: AFML,
Technical Library

1 Attn: AFML/LLD,
Dr. T.M.F. Ronald

Federal Aviation Administration
800 Independence Avenue, S.W.
Attn: Admin Standard Division
Washington, DC 20590

Director
Advanced Research Projects Agency
Department of Defense
Washington, DC 20301

Director
National Bureau of Standards
Washington, DC 20025

National Academy of Science

Attn: Dr. J.R. Lane
2101 Constutution Avenue, N.W.
Washington, DC 20418

National Aeronautics & Space
Administration
Attn: Code RRM
Federal Buildg #10
Washington, DC 20456

## DISTRIBUTION (Cont'd)

US Atomic Energy Commission
Document Library
Germantown, MD  21403

Director
US Army Air Mobility Research &
    Development Laboratory
Ames Research Center
Attn:  Mr. Paul Yaggy
Moffet Field, CA  94035

Defense Documentation Center  (12)
Cameron Station
Alexandria, VA  22314

Frankford Arsenal:

1 Attn:  AOA-M/107-B

1 Attn:  TD/107-1

1 Attn:  MD/220-1

1 Attn:  MT/211-2

1 Attn:  QAA-R/235-3

1 Attn:  PA/107-2

1 Attn:  GC/28-1

1 Attn:  PD/64-4
         Mr. George White

5 Attn:  PDM-E/64-3
         P. Gordon

5 Attn:  PDM-E/64-3
         F. Lee

1 Attn:  PDM-A/64-2

1 Attn:  PDM-E/64-4
         Project File

1 Attn:  MDA-D/220-3
         K. Ryan

1 Attn:  MDA-D/220-3
         D. Lenton

10 Attn:  PDM-E/64-4
          M. Schwartz

1 Attn:  MDC/219-2

1 Attn:  MDS/220-2

1 Attn:  MDS-S/220-2

1 Attn:  MDA/220-3

1 Attn:  MDA-D/220-3

1 Attn:  MDA-D/220-3
         K. Pitko

3 Attn:  TSP-L/51-2
         (1 - Circulation copy
          1 - Reference copy
          1 - Record copy)

Printing & Reproduction Division
FRANKFORD ARSENAL
Date Printed: 17 November 1975

**DEPARTMENT OF THE ARMY**
FRANKFORD ARSENAL
PHILADELPHIA, PA. 19137

OFFICIAL BUSINESS
PENALTY FOR PRIVATE USE $300